RSC Advances

ROYAL SOCIETY OF CHEMISTRY

www.rsc.org/advances

View Article Online
DOI: 10.1039/C3RA46132G

Palladium-based Micellar Nanohybrids: Preparation and Nonlinear Optical Response

Irene Papagiannouli[a,b], Maria Demetriou[c], Theodora Krasia-Christoforou[c]* and Stelios Couris[a,b]*

[a]Department of Physics, University of Patras, Patras 26504, GREECE
[b]Institute of Chemical Engineering Sciences (ICEHT), Foundation for Research and Technology-Hellas (FORTH), P.O. Box 1414, Patras 26504, GREECE
[c]Department of Mechanical and Manufacturing Engineering, University of Cyprus, P.O. Box 20537, 1678 Nicosia, CYPRUS

submitted for publication in *RSC Advances*

Revised January 2014

*Corresponding authors e-mails: krasia@ucy.ac.cy, couris@iceht.forth.gr

View Article Online
DOI: 10.1039/C3RA46132G

Abstract

In the present work the synthesis and physicochemical characterisation of a new class of Pd-containing micellar nanohybrid systems are presented. The new systems consist of metallic Pd nanoparticles and well-defined diblock copolymers, possessing carbazole and *β*-ketoester side-chain functionalities namely poly[2-(N-carbazolyl) ethyl methacrylate]-*block*-poly[2-(acetoacetoxy) ethyl methacrylate] ($CbzEMA_x$-*b*-$AEMA_y$). Block copolymer synthesis has been carried out by Reversible Addition-Fragmentation chain Transfer (RAFT) polymerisation. The presence of the *β*-ketoester groups within these diblock copolymers enabled the complexation and stabilisation of the Pd nanoparticles in tetrahydrofuran. Visualisation of the Pd-containing micellar nanohybrids was realised by means of transmission electron microscopy (TEM), providing information on the metal nanoparticle sizes. The nonlinear optical response of these polymer-metal nanohybrid systems has been systematically studied both in solution and in thin films, using the Z-scan technique, employing 35 ps, visible (532 nm) and infrared (1064 nm) laser excitation. Discussion in regards to the spectral position of the surface plasmon resonance (SPR) of the Pd nanoparticles and its effect on the nonlinear optical response of the micellar systems has been carried out in terms of two photon process.

View Article Online
DOI: 10.1039/C3RA46132G

1. Introduction

Polymer-based materials exhibiting interesting optical and electronic properties have attracted significant attention due to their potential use in various applications including organic-based photovoltaics[1,2], polymer light emitting diodes[3], thin film transistors and sensors[4], optical switching[5], optical data storage and information processing[6,7].

Carbazole-containing polymers in which the carbazole unit is located in either the main or in the side chain, belong to one of the most investigated systems in the area of polymer-based optoelectronic materials[8]. Such materials present good electro- and photoactive properties, high charge carrier mobilities, hole transporting capability and electroluminescent properties. Moreover, these materials are characterised by high thermal, chemical and environmental stability. As a result, there are many reports in the literature concerning the photorefractive and nonlinear optical (NLO) properties of carbazole-containing polymers. As an example, Fuks *et al.* have investigated the third-order NLO properties of poly(N-vinylcarbazole) by means of degenerate four-wave mixing (DFWM) employing visible laser excitation[9]. Zhang and co-workers have investigated the optical properties of main chain polymers containing carbazole NLO-phores[10]. Moreover, Zhan *et al.* have studied the off-resonant third order NLO response of conjugated copolymers containing carbazole and fluorine groups *via* DFWM measurements under infrared excitation[11].

During the last years, metal nanoparticles (NPs) have also attracted considerable attention because of their size-dependent properties, their high surface-to-volume ratios and their plasmonic effects, all these characteristics contributing to very interesting chemical and electrochemical properties. Consequently, NPs are among the most promising candidates for several applications in photonics, optoelectronics, sensing, catalysis etc. In particular, concerning applications related to the optical properties of NPs, the most investigated systems have been noble metals[12,13] and semiconducting[14-16] NPs.

A promising strategy for the development of new materials exhibiting attractive optoelectronic properties is the combination of electro-optical polymers with NPs. In that view, the combination of polymers with transition NPs[17,18] has attracted the scientific interest very recently. Palladium (Pd) characterised by nanoscale

View Article Online
DOI: 10.1039/C3RA46132G

dimensions is considered to be one of the most attractive metals since besides its NLO properties that are relatively unexplored and rather poorly understood[19-22], it also exhibits very interesting catalytic, hydrogen storage[23] and sensing properties[24,25]. The use of well-defined nanostructured domains such as amphiphilic block copolymer micelles as stabilisers for Pd nanoparticles in solution provides an ideal nano-environment for the controlled nanoparticle formation and NP localisation in the nanoscale[26].

Recently we have been focusing on the synthesis and characterisation of micellar organic-inorganic nanohybrids based on a relatively new family of coordination copolymers bearing *β*-ketoester side chain functionalities[27,28]. Our initial studies on the investigation of the NLO response were performed on nanohybrid systems based on diblock copolymer micelles consisting of a highly hydrophobic monomer namely lauryl methacrylate (LauMA) and the metal chelating monomer 2-(acetoacetoxy) ethyl methacrylate (AEMA) employed for the complexation and stabilisation of Pd NPs in n-hexane. These systems have been found to exhibit rather low third-order susceptibility $\chi^{(3)}$ values when excited with 35 ps laser light in the visible or in the infrared, while their NLO response was found to remain unaffected by changing the size of the encapsulated Pd NPs [29].

In an effort to develop new polymer-based hybrid nanomaterials with enhanced optical nonlinearity, a new block copolymer family has been synthesised in which the AEMA metal binding groups are combined with 2-(N-carbazolyl) ethyl methacrylate (CbzEMA) units. A simple and cost-effective synthetic approach involving Reversible Addition Fragmentation chain Transfer (RAFT) polymerisation has been employed towards this purpose[30].

For the first time AEMA is combined with CbzEMA to yield well-defined functional diblock copolymers presenting electroactive and metal chelating properties. Hence, the present work describes the unique combination of a relatively rare example of a metal chelating monomer polymerised by RAFT, with an electro- and photoactive polymethacrylate, the controlled polymerisation of which has been rarely reported[31-34]. The RAFT process was readily employed to prepare well-defined $CbzEMA_x$ homopolymers and $CbzEMA_x$-*b*-$AEMA_y$ diblock copolymers, that were further characterised in regards to their molecular and compositional features. The

View Article Online
DOI: 10.1039/C3RA46132G

$CbzEMA_x$-*b*-$AEMA_y$ diblock copolymers were further used as macromolecular steric stabilisers for Pd NPs in organic media resulting in the generation of Pd-containing block copolymer micelles. To the best of our knowledge, this is the first systematic investigation of the NLO properties of these nanohybrids in the infrared (1064 nm) and in the visible (532 nm) regions under 35 ps laser excitation, both in solution and in thin films.

2. Experimental

Materials and Methods

Benzene (Fluka, ≥ 99.5%) and tetrahydrofuran (THF) (Scharlau, 99.9%) were stored over CaH_2 (Merck, 99.9%) and distilled under reduced pressure immediately prior to the polymerisation reactions. Methanol (LabScan, 99.9%), n-hexane (LabScan, 99%), toluene (Scharlau, 99.9%), dimethylformamide (DMF) (Aldrich, 99.8%), cyclohexane (Sigma-Aldrich, ≥ 99.9%), dichloromethane (Sigma-Aldrich, ≥ 99.5%), HCl (Merck, 37% solution), diethyl ether (LabScan, 99.5%), benzoic acid (Merck, 99%), aqueous solution of tetrabutylammonium hydroxide (Sigma-Aldrich, 40% w.t.), triethylamine (Merck, ≥ 99%), hydrazine monohydrate (Sigma-Aldrich, 98%), benzyl chloride (Sigma-Aldrich, 99%), carbon tetrachloride (Riedel de Haën, ≥ 99.8 %), α-methylstyrene (Sigma-Aldrich, 99%), sodium methoxide (Aldrich, 30% solution in methanol), carbazole (Sigma, ≥ 95%), ethylene carbonate (Aldrich, ≥ 98%), methacryloyl chloride (Fluka, ≥ 97%) and deuterated chloroform (Merck) were used as received. The following inorganic compounds were used without further purification: Sulfur (Aldrich, powder ~ 100 mesh), silica gel (Aldrich, 60 Å, 70-230 mesh), NaOH pellets (Scharlau, 99%), KOH pellets (HiMedia, 85%), Na_2SO_4 (HiMedia, 99%), $NaHCO_3$ (Sigma-Aldrich, 99.5%), NaCl (HiMedia, ≥ 99.0%), $Pd(CH_3COO)_2$ (Sigma-Aldrich, 99.98%), anhydrous $MgSO_4$ (Scharlau, 98%). 2-(acetoacetoxy) ethyl methacrylate (AEMA) (Sigma-Aldrich, 95%) was passed through a basic alumina column prior to the polymerisations and used without further purification. 2,2-Azobis(isobutylnitrile) (AIBN) (Sigma-Aldrich, 95%) was recrystallised twice from ethanol and dried under vacuum at room temperature for three days. Cumyl dithiobenzoate (CDTB) was synthesised following a procedure reported by Le *et al.*[35].

View Article Online
DOI: 10.1039/C3RA46132G

Synthesis

2-(N-carbazolyl) ethyl methacrylate (CbzEMA). The synthesis of the monomer CbzEMA was performed in two steps by following a modified methodology reported in the literature[31,36,37]. A DMF solution of carbazole (19 g, 0.114 mol) and ethylene carbonate (11 g, 0.125 mol) was placed under reflux for 8h in the presence of KOH (1.9 g). After been cooled down to room temperature, the reaction mixture was filtered and then poured into a large amount of water (4 L). The precipitated white crystalline 2-(N-carbazolyl) ethanol (yield: 38%) was collected and dried in a vacuum oven for 12h at 40 ^{o}C. Subsequently, it was recrystallised twice in a 1:1 v/v benzene/cyclohexane mixture.

The purified 2-(N-carbazolyl) methanol (5 g, 0.024 mol) was then dissolved in dichloromethane (80 mL). In the reaction flask, triethylamine (2.8 mL, 0.028 mol) and methacryloyl chloride (4 mL, 0.028 mol) were added. The addition of triethylamine and methacryloyl chloride was carried out in a 20% excess, for a more quantitative reaction. The methacryloyl chloride was added dropwise during stirring at 0 ^{o}C. During the addition, an exotherm was observed and sediment was formed, namely hydrochloric triethylamine (Et_3NHCl), which is a by-product of the reaction. The reaction mixture was stirred for 24h. The hydrochloric triethylamine was filtered off by using a glass frit filter. After filtration, water (10 mL) was added in the mixture for the hydrolysis of the excess methacryloyl chloride into methacrylic acid and the segregation of the organic phase from the aqueous. The product remained in the organic phase. Subsequently, dichloromethane (40 mL) was added in the solution and the mixture was extracted two times with water (5 and 10 mL), then three times with $NaHCO_3$ solution (5% in water, 3 x 5 mL) and again three times with water (3 x 5 mL). The obtained monomer was recrystallised twice in methanol (yield: 42%).

^{1}H NMR (300MHz, $CDCl_3$) δ (ppm): 8.1 (d, - carbazole aromatic protons), 7.46 (m, - carbazole aromatic protons), 7.24 (m, - carbazole aromatic protons), 5.92 (s, $=CH_2$), 5.48 (s, $=CH_2$), 4.64 (t, $N–CH_2$), 4.53 (t, $O–CH_2$), 1.94 (s, CH_3).

CbzEMA homopolymers. CbzEMA (733 mg, 2.63 mmol) was placed in a round-bottom flask and dissolved in freshly distilled benzene (0.7 mL) under a dry nitrogen atmosphere. CDTB (7.2 mg, 0.026 mmol) and AIBN (2.36 mg, 0.014 mmol) dissolved in benzene were then transferred into the flask *via* a syringe. The reaction mixture was degassed by three freeze–evacuate–thaw cycles and placed under a dry

View Article Online
DOI: 10.1039/C3RA46132G

nitrogen atmosphere at 65 ^{o}C for 20h. The polymerisation was terminated by cooling the reaction down to room temperature. The produced homopolymer (555 mg, 76% polymerisation yield) was retrieved by precipitation in methanol and was left to dry under vacuum at room temperature for 24h.

^{1}H NMR (300MHz, $CDCl_3$) δ (ppm): 7.1-7.9 (s, -Ph), 4.15 (s, N-CH_2), 3.98 (s, O-CH_2), 1.6 (s, -CH_2), 0.86 (m, -CH_3).

CbzEMA$_x$-*b*-AEMA$_y$ diblock copolymers. In a round-bottom flask, the macro-CTA, $CbzEMA_{82}$, (Mn^{SEC}=23075 g.mol^{-1}, 493 mg, 0.020 mmol) was placed and dissolved in freshly distilled THF (0.9 mL) under a dry nitrogen atmosphere. AIBN (1.6 mg, 0.0096 mmol) dissolved in THF and AEMA (0.2 ml, 0.99 mmol) were then transferred into the flask *via* a syringe. The reaction mixture was degassed by three freeze–evacuate–thaw cycles and placed under a dry nitrogen atmosphere at 65 ^{o}C for 20 hours. The polymerisation was terminated by cooling the reaction down to room temperature. The produced diblock copolymer (603 mg, 36% polymerisation yield) was retrieved by multiple precipitations in methanol and was left to dry under vacuum at room temperature for 24 hours.

^{1}H NMR (300MHz, $CDCl_3$) δ (ppm): 7.9 (br, -Ph), 7-7.2 (br, -Ph), 4.35 (br, -CH_2), 4.18 (br, N-CH_2), 3.97 (s, O-CH_2), 3.75 (br, -CH_2), 3.56 (br, -CH_2), 2.29 (br, -CH_3), 0.86-2.00 (m, -CH_2, -CH_3).

CbzEMA$_x$-*b*-AEMA$_y$/Pd(^{0}) micellar nanohybrids. $CbzEMA_{82}$-*b*-$AEMA_{47}$ (20 mg, 0.0284 mmol of AEMA units) was dissolved in THF (5 mL). After complete dissolution of the polymer, triethylamine (40μL, 0.2870 mmol) was added to the solution. Subsequently, the resulting solution was transferred in a glass vial containing $Pd(CH_3COO)_2$ (3.2 mg, 0.0142 mmol) and left to stir at room temperature until complete solubilisation of the salt. Finally, hydrazine monohydrate was added to the solution upon stirring. The reduction of Pd(II) ions to noble Pd was accompanied by a color change of the solution from yellow to dark brown.

Film fabrication. The Pd-containing micellar nanohybrids were spin-coated on glass substrates using a Schaefer-Tech AG/SCI-50 spin-coater. The spin velocity was 4500

View Article Online
DOI: 10.1039/C3RA46132G

rpm and the spinning time 40 sec. Selected films have been also annealed at 170 ^{o}C for 1 hour.

Characterisation Methods

NMR spectra were recorded in $CDCl_3$ using an Avance Brucker 300 MHz spectrometer equipped with an Ultrashield magnet. Tetramethylsilane (TMS) was used as an internal reference in $CDCl_3$. The molecular weights and molecular weight distributions (MWD) of the polymers were determined by size exclusion chromatography (SEC) using equipment supplied by Polymer Standards Service (PSS). All measurements were carried out at room temperature using Styragel HR 3 and Styragel HR 4 columns. The mobile phase was THF, delivered at a flow rate of 1 mL min^{-1} using a Waters 515 isocratic pump. The SEC data were obtained using a refractive index detector (Waters 2414) supplied by PSS. The instrumentation was calibrated using poly(methyl methacrylate) (PMMA) standards with narrow polydispersity indices (MWs of 102, 450, 670, 1580, 4200, 14400, 31000, 65000, 126000, 270000, 446000, 739000 g mol^{-1}) supplied by PSS. Dynamic Light Scattering (DLS) measurements were carried out using a DLS 90Plus Brookhaven scattering spectrometer operating at 633 nm (power: 30 mW). DLS experiments were performed at a 90^{o} scattering angle**.** Solution concentrations maintained at 1g/L. All polymer solutions were filtered through PTFE microfilters (pore size: 0.45 μm) prior to measurements. Transmission electron microscopy (TEM) studies were performed on a 1010 JEOL microscope (200 kV). The micellar solutions were left to dry on a carbon coated copper grid to allow the TEM investigation.

The nonlinear optical properties of the Pd-containing micellar systems have been studied be means of the Z-scan technique[38], which can provide simultaneously the sign and the magnitude of the nonlinear absorption and refraction of a sample. Briefly, during the Z-scan measurements, the sample moves through the focal plane, along the propagation direction of a focused laser beam, thus experiencing different laser intensity at each position. The transmitted laser beam is then divided in two parts, e.g. by a beam splitter, allowing two different experimental configurations, the so-called “open” and “closed-aperture” Z-scans respectively. In the former configuration, the transmitted laser light is totally collected (e.g. using a large diameter lens), while in the latter, only a part of the transmitted laser beam is

View Article Online
DOI: 10.1039/C3RA46132G

collected, after it has passed through a small aperture placed in the far field. From the division of the "closed-aperture" Z-scan recording by the corresponding "open-aperture" one, the so-called "divided" Z-scan is obtained, from which the total variation of the transmission, i.e. the ΔT_{pv}, is determined. This last quantity is related to the on-axis nonlinear phase shift $\Delta\Phi_0$ through the following relation:

$$\left|\Delta\Phi_0\right| = \frac{\Delta T_{pv}}{0.406(1-S)^{0.27}} \tag{1}$$

where S is the fraction of beam transmitted through the aperture. Then, the nonlinear refractive index parameter γ' can be deduced through the relation:

$$\gamma' = \frac{\Delta\Phi_0}{kI_0 L_{eff}} \tag{2}$$

where I_0 is the laser peak intensity at the focus, $L_{eff} = 1-\exp(-a_0 L)/a_0$ is the effective path length of the sample which is related to the linear absorption coefficient α_0 of the sample and the sample thickness L and $k=2\pi/\lambda$ is the wave vector.

From the "open-aperture" Z-scan the nonlinear absorption coefficient β can be obtained by fitting with the following relation[38]:

$$T = \sum_{m=0}^{\infty} \frac{\left[-q_0(0,0)\right]^m}{(m+1)^{3/2}} \tag{3}$$

where $q_0(0,0) = \beta I_0 L_{eff}$. Finally, with the parameters β and γ' known, the real ($\mathrm{Re}\chi^{(3)}$) and the imaginary ($\mathrm{Im}\chi^{(3)}$) parts of the third-order nonlinear susceptibility can be easily calculated using the following relations:

$$\mathrm{Re}\,\chi^{(3)}(esu) = \frac{c(m/s)\,n_0^2\,\gamma'(m^2/W)}{480\,\pi^2} \tag{4}$$

$$\mathrm{Im}\,\chi^{(3)}(esu) = \frac{c^2(m/\mathrm{s})^2\,n_0^2\,\beta(m/W)}{960\,\pi^2\,\omega(\mathrm{s}^{-1})} \tag{5}$$

View Article Online
DOI: 10.1039/C3RA46132G

where n_0 is the linear refractive index (which is the refractive index of the solvent in the case of solutions), c is the speed of light, ε_0 is the permittivity of free space and ω is the angular frequency of the laser radiation.

For the measurements a 35 ps mode-locked Nd:YAG laser (Quantel YG900) operating at 1064 and 532 nm, at a repetition rate of 10 Hz was employed. A more detailed description of the analysis of the experimental data can be found elsewhere[39,40]. The solutions of the investigated Pd-containing micellar samples were placed into 1 mm thick quartz cells while their UV-Vis-NIR optical absorption spectra were regularly measured by a spectrophotometer (Hitachi U3000), in order to ensure that no photo-degradation has occurred during the measurements. The laser beam was focused in the sample by means of a 20 cm focal length quartz lens.

3. Results and discussion

Figure 1 illustrates the chemical structures and names of the two monomers and the chain transfer agent (CTA) used in polymer synthesis.

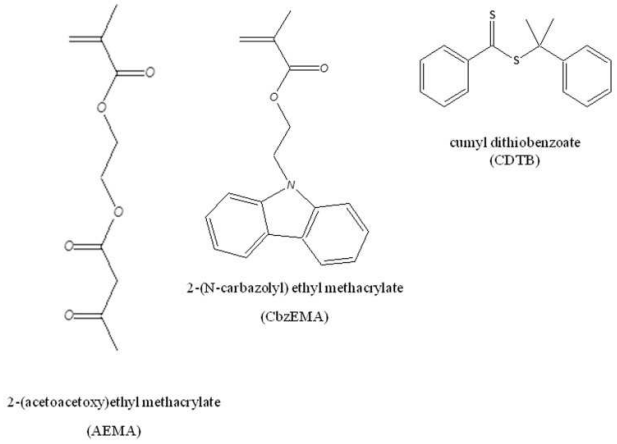

Fig. 1 Chemical structures of the two monomers (AEMA and CbzEMA) and the CTA (CDTB) used in polymer synthesis.

Molecular weights and composition of the $CbzEMA_x$ homopolymers and the $CbzEMA_x$-*b*-$AEMA_y$ diblock copolymers. $CbzEMA_x$ homopolymers and $CbzEMA_x$-*b*-$AEMA_y$ diblock copolymers were successfully synthesised following

View Article Online
DOI: 10.1039/C3RA46132G

typical RAFT methodologies already described in the Experimental Section. The molecular characterisation of these materials was carried out by means of size exclusion chromatography (SEC) and proton nuclear magnetic resonance spectroscopy (^{1}H NMR). Table 1 summarises the chemical structures of all homopolymers and diblock copolymers prepared in this study along with their molecular weight (MW) and composition characteristics. Narrow to moderate molecular weight distributions (MWD) – defined as the ratio of the weight average (M_w) to the number average (M_n) molecular weight – were observed for the homopolymers and diblock copolymers, varying between ~1.2 – 1.5.

Table 1 Characteristics of the homopolymers and block copolymers based on CbzEMA and AEMA obtained by RAFT (conversion percentages, molecular weights and molecular weight distributions (MWD)).

Experimental Structure[a]	Conversion (%)	Theor. MW[b] gmol^{-1}	SEC[c] M_n (gmol^{-1})	MWD
$CbzEMA_{82}$	76	21388	26590	1.23
$CbzEMA_{82}$-*b*-$AEMA_{47}$	36	33374	31800	1.31
$CbzEMA_{104}$	75	41830	29158	1.50
$CbzEMA_{104}$-*b*-$AEMA_{44}$	n.d.	n.d.	22950	1.33
$CbzEMA_{38}$	81	11534	10883	1.22
$CbzEMA_{38}$-*b*-$AEMA_{50}$	75	12483	12561	1.34

[a]determined by SEC and ^{1}H NMR; [b][(g. monomer)/(mol RAFT agent)]×(polymerisation yield) + MW of CTA (for homopolymers) and [(g. monomer)/(mol CTA agent)]x(polymerisation yield) + M_n of macro-CTA (for diblock copolymers); [c]SEC calibrated with PMMA standards; M_n = number average molecular weight; MWD = molecular weight distribution; CbzEMA = 2-(N-carbazolyl) ethyl methacrylate; AEMA = 2-(acetoacetoxy)ethyl methacrylate; n.d.: not determined.

The expected chemical structure of the $CbzEMA_x$-*b*-$AEMA_y$ diblock copolymers was confirmed by ^{1}H NMR spectroscopy. Fig. 2 exemplarily shows the ^{1}H NMR spectrum of the $CbzEMA_{82}$-*b*-$AEMA_{47}$ diblock copolymer. The peak assignments are shown in the spectrum. The AEMA comonomer compositions were determined from the ratio

View Article Online
DOI: 10.1039/C3RA46132G

of the areas under the characteristic signals of the AEMA and the CbzEMA, appearing at 2.27 (f) and 7.9 (h) respectively.

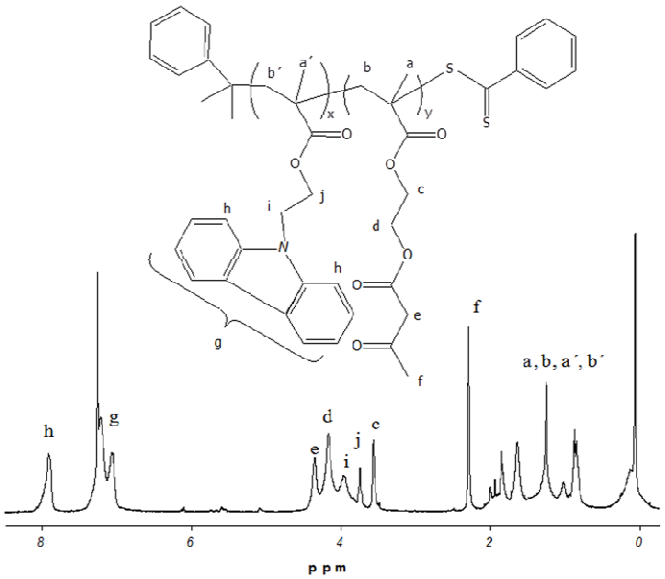

Fig. 2 ^{1}H NMR spectrum of the CbzEMA$_{82}$-*b*-AEMA$_{47}$ diblock copolymer recorded in $CDCl_3$.

CbzEMA$_x$-*b*-AEMA$_y$/Pd(^{0}) micellar nanohybrids. The CbzEMA$_x$-*b*-AEMA$_y$/Pd(^{0}) hybrid micelles were prepared in tetrahydrofuran (THF). The latter is a non-selective solvent (i.e. a good solvent) for both, the CbzEMA and AEMA block segments. Therefore, the CbzEMA$_x$-*b*-AEMA$_y$ block copolymers exist only as unimers in this solvent in the absence of the Pd NPs. Micellisation is induced upon the addition of the $Pd(CH_3COO)_2$ in the solution followed by reduction in the presence of hydrazine monohydrate, as schematically depicted in Fig. 3.

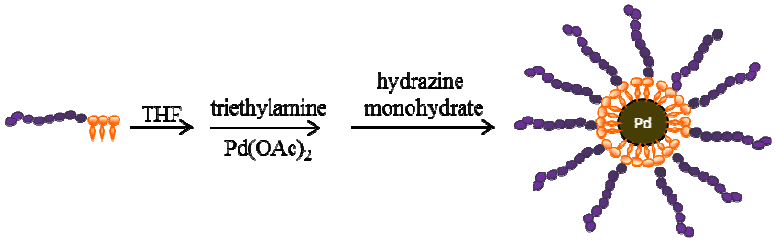

Fig. 3 Formation of micellar nanohybrids consisting of CbzEMA$_x$-*b*-AEMA$_y$ diblock copolymers and Pd NPs in an organic solvent (THF).

View Article Online
DOI: 10.1039/C3RA46132G

Similar observations i.e. micelle formation upon complexation and/or reduction have been reported by various groups. For example, L. M. Bronstein *et al*. have reported on the formation of micellar structures in aqueous media upon interaction of certain metal compounds such as Pd, Au and Pt with poly(ethylene oxide)-*b*-poly(ethylene imine) double-hybrophilic block copolymers[41]. Moreover, H. Zhao and co-workers have reported on the induction of micellisation in THF upon coordination of Cd^{2+} metal ions with the 2VP units of poly(styrene-*b*-2-vinylpyridine) (PS-*b*-P2VP) block copolymer. In the absence of the ions both block segments are soluble in THF, i.e. no micelles are present, whereas, upon the addition of Cd^{2+} to the PS-*b*-P2VP/THF solution, complexed 2VP segments become insoluble in THF and collapse resulting to micelle formation[14].

Dynamic Light Scattering (DLS) was used for determining the hydrodynamic diameters (D_H) of the $CbzEMA_{82}$-*b*-$AEMA_{47}$ and $CbzEMA_{104}$-*b*-$AEMA_{44}$ hybrid micelles that were further investigated in respect to their NLO response in solution. The obtained results are summarised in Table 2.

Table 2 Hydrodynamic diameters of the $CbzEMA_x$-*b*-$AEMA_y$ micellar nanohybrids generated in THF after the addition of $Pd(CH_3COO)_2$ followed by reduction.

Experimental Structure	**$CbzEMA_{82}$ -*b*-$AEMA_{47}$**	**$CbzEMA_{104}$-*b*-$AEMA_{44}$**
D_H (theoretical)*	66	75
D_H (no Pd) (nm)	~ 3	~ 3
D_H (nm) [AEMA:$Pd(^0)$]=2:1	72	91
D_H (nm) [AEMA:$Pd(^0)$]=1:1	91	114

*assuming the generation of micelles with spherical morphology and fully-extended chains

As seen in Table 2, upon increasing the inorganic content within the micelles, the hydrodynamic diameter increases. As previously reported[41], in cases where micelles are formed owing to complexation with a metal compound, a change in metal loading may significantly affect the micellar size. The obtained D_H values exceed the maximum theoretical micelle diameters calculated assuming spherical morphology and fully-extended chains, suggesting the presence of micellar aggregates in solution.

View Article Online
DOI: 10.1039/C3RA46132G

The latter is also confirmed by TEM analysis. Exemplarily, TEM images of $CbzEMA_x$-*b*-$AEMA_y$ micellar aggregates having Pd NPs incorporated within their cores are presented in Fig. 4. Using the Digimizer Image Analysis Software, the average particle sizes were calculated to be 63.9 ± 10 nm for the $CbzEMA_{82}$-$AEMA_{47}$ /Pd(^{0}) (1:1) system and 78.5 ± 9 nm for the $CbzEMA_{104}$-$AEMA_{44}$ /Pd(^{0}) (2:1) system.

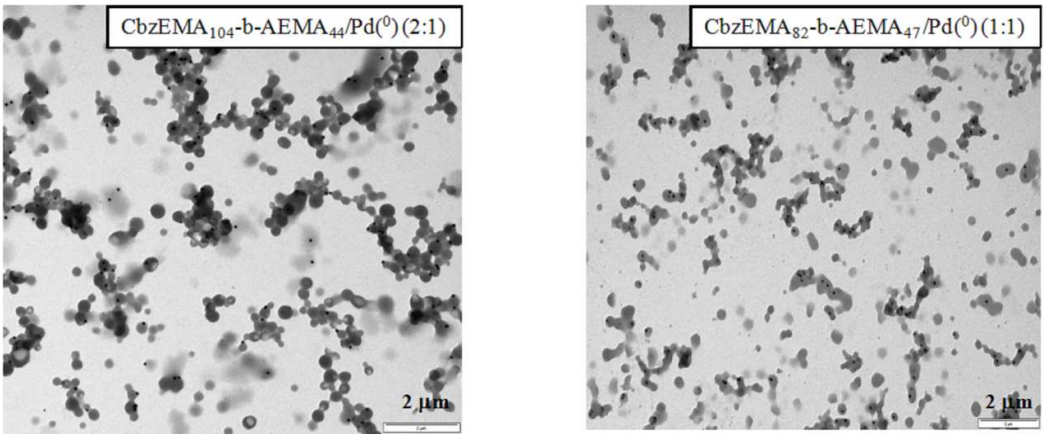

Fig. 4 TEM images of $CbzEMA_x$-*b*-$AEMA_y$/Pd(^{0}) micellar nanohybrids generated in THF.

Nonlinear Optical (NLO) Properties. For the determination of the NLO properties of the Pd-containing micellar nanohybrid systems, various solutions with different $CbzEMA_{82}$-*b*-$AEMA_{47}$/Pd(^{0}) and $CbzEMA_{104}$-*b*-$AEMA_{44}$/Pd(^{0}) concentrations in THF have been prepared. In addition, Pd-containing micellar systems with different polymer-to-metal molar ratios (i.e. AEMA to Pd) have been synthesised and investigated, called hereafter 1:1 and 2:1 systems, with the 2:1 micellar systems containing half of the Pd load compared to the 1:1 ones. The NLO properties of the prepared systems have been investigated under both visible (532 nm) and infrared (1064 nm), 35 ps laser excitation. Some representative UV-Vis-NIR absorption spectra of the prepared micellar solutions are presented in Fig. 5, together with the absorption spectrum of the pristine copolymer $CbzEMA_{82}$-*b*-$AEMA_{47}$ for comparison purposes. As seen from the spectra, the copolymer was found to exhibit negligible absorption in the visible and near infrared, while the Pd-containing micelles exhibited sizeable absorption, this difference attributed to the Pd presence in the micellar nanohybrid systems. As a matter of fact, the absorption spectra of the samples shown in Fig. 5, having the same Pd concentration (i.e. 1 mM), exhibited the same absorbance in the 400 to 800 nm spectral range, independently of the copolymer type

View Article Online
DOI: 10.1039/C3RA46132G

employed. For these reasons, in the next, the reported samples' concentrations will be referred to the Pd content of each solution instead of the concentration of the Pd-containing micellar entities in solution.

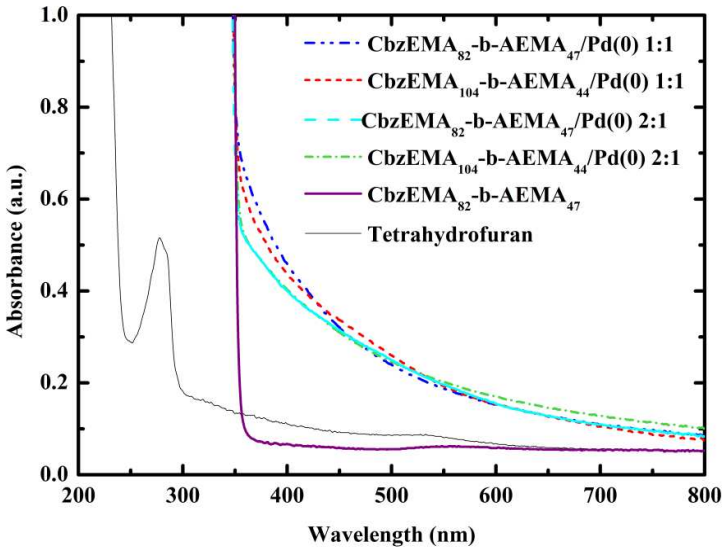

Fig. 5 UV-Vis-NIR absorption spectra of the copolymer $CbzEMA_{82}$-*b*-$AEMA_{47}$, and the $CbzEMA_{82}$-*b*-$AEMA_{47}/Pd(^0)$ and $CbzEMA_{104}$-*b*-$AEMA_{44}/Pd(^0)$ micellar solutions in THF.

In order to check if the observed NLO response had contributions arising from the solvent and/or the copolymer, Z-scan measurements of the neat solvent (i.e. THF) and of various concentration' solutions of the $CbzEMA_x$-*b*-$AEMA_y$ copolymers in THF were performed, at both excitation wavelengths, under identical experimental conditions to those used for the investigation of the Pd-containing micellar systems. In all cases, the $CbzEMA_x$-*b*-$AEMA_y$ copolymer solutions exhibited negligible NLO response for the range of incident laser energies used, whereas THF exhibited only nonlinear refraction, which was measured separately in order to be taken into account for the determination of the nonlinear response of the Pd-containing micellar solutions. The magnitude of the third-order susceptibility $\chi^{(3)}$ of THF was determined to be $(2.8\pm0.6)\times10^{-22}$ and $(2.5\pm0.2)\times10^{-22}$ m^2/V^2 under 35 ps, 532 and 1064 nm laser excitation respectively in very good agreement with other published reports[42,43].

The present study has revealed that the investigated micellar nanohybrid systems had substantial NLO response, comparable to that reported recently in another study of similar systems, where a different block copolymer, namely the poly(lauryl

View Article Online
DOI: 10.1039/C3RA46132G

methacrylate)-*block*-poly(2-(acetoacetoxy) ethyl methacrylate) ($LauMA_x$-*b*-$AEMA_y$)[29] has been employed. In particular, the $LauMA_x$-*b*-$AEMA_y$/Pd micellar systems were found to exhibit both nonlinear absorption and refraction when excited with 532 and 1064 nm laser light.

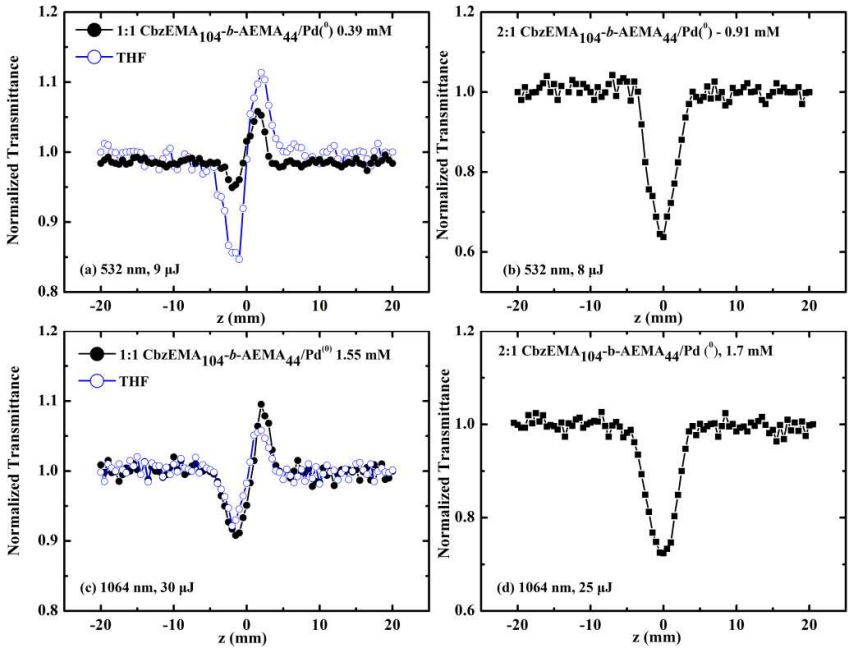

Fig. 6 Representative "divided" and "open-aperture" Z-scans of THF Pd-containing micellar nanohybrid solutions, under 35 ps, 532 nm (a, b) and 1064 nm (c, b) laser excitation.

In Figure 6b, the "open-aperture" Z-scan recording of a 0.91 mM solution of the 2:1 $CbzEMA_{104}$-*b*-$AEMA_{44}$/Pd(^{0}) micellar system, measured under 532 nm excitation is shown. As shown, this micellar system was found to exhibit important transmission minimum suggesting the presence of strong nonlinear absorption. Similar behaviour was observed for the other micellar systems as well. Similarly, important nonlinear absorption was observed under infrared excitation as shown from the "open-aperture" Z-scans in Fig. 6d, corresponding to a 1.7 mM 2:1 $CbzEMA_{104}$-*b*-$AEMA_{44}$/Pd(^{0}) micellar system solution. It should be mentioned at this point that in all infrared excitation measurements, significantly larger laser energies and concentrations were used compared to those used under visible excitation. Based on these experimental

View Article Online
DOI: 10.1039/C3RA46132G

evidences, it can be reasonably assumed that under visible excitation, a resonance enhancement should be operational. In addition, all Pd-containing micellar nanohybrid systems have been found to exhibit positive sign nonlinear absorption, corresponding to reverse saturable like behaviour (RSA) both in the visible and in the infrared.

Concerning the nonlinear refraction of the micellar nanohybrids, from the analysis of the Z-scan data, it was concluded that the Pd-containing micellar systems and the solvent exhibited opposite sign nonlinear refraction under visible excitation, while they exhibited same sign nonlinear refraction under infrared excitation. As a matter of fact, since THF exhibited valley-peak transmission configuration, indicating positive sign nonlinear refraction (i.e. self-focusing) at both excitation wavelengths as shown by the shape of the corresponding Z-scan recordings presented in Fig. 6a and 6c, it becomes evident that the micellar systems should exhibit negative nonlinear refraction, (i.e., self-defocusing) under 532 nm excitation and positive nonlinear refraction (i.e., self-focusing) under 1064 nm excitation.

In conclusion, the micellar nanohybrids were found to exhibit both nonlinear refraction and absorption under both visible and infrared excitation conditions, while their nonlinear refraction under infrared excitation was significantly weaker to that observed under visible excitation from similar concentration solutions. In general, both the nonlinear refraction and absorption were found to be more important in the visible than in the infrared, indicating most probably the presence of resonance enhancement. In all cases, the analysis of the Z-scan measurements revealed $\chi^{(3)}/ a_0$ values ranging between $(7\text{-}18.2)\times10^{-25}$ m^3/V^2 in the visible and $(1.4\text{-}2.\ 1)\times10^{-25}$ m^3/V^2 in the infrared, while a good linear dependence of the $\chi^{(3)}$ *versus* Pd content was obtained, with no significant dependence with the size and the $AEMA_y$ to $Pd(^0)$ ratio. These experimental findings could be attributed to the fact that the Pd NPs generated within the cores of the different micellar systems, did not exhibit any significant size differences (based on TEM data), thus resulting to similar $\chi^{(3)}$ values regardless of the hydrodynamic micellar size. This is in agreement with some recent results suggesting similar weak dependence of the NLO response on the size of Pd core encapsulated within the block copolymer micelles, under both visible and infrared laser excitation[44].

View Article Online
DOI: 10.1039/C3RA46132G

In a recent study[19], the NLO properties of commercially available Pd NPs in colloidal suspensions in water and ethanol, with sizes of about 3-5 nm have been reported. The excitation was performed using 792 nm, 120 fs and 210 ps laser light. In the case of excitation using the 210 ps laser pulses, which are more relevant to the present experimental conditions, a positive sign nonlinear refractive index of 9×10^{-15} m^2W^{-1} and negligible nonlinear absorption have been observed. Similarly, in another study, investigating the NLO properties of similar Pd suspensions, using 1064 nm, 50 ps laser excitation, negative nonlinear refraction and positive nonlinear absorption have been reported[45]. In particular, the nonlinear refractive parameter γ' and the nonlinear absorption coefficient β were determined to be -1.2×10^{-19} m^2W^{-1} and 5.4×10^{-13} mW^{-1} respectively for a 20 mM Pd suspension. From the above, it becomes evident that despite the disagreement about the sign of the nonlinear refraction, a quite satisfactory agreement exists concerning the magnitude of both the refractive and absorptive parts of the third-order optical nonlinearity.

In order to further investigate the NLO properties of the Pd-containing nanohybrids and shed more light on the issue of the controversial literature results concerning the sign of the nonlinear refraction, thin films of these micellar systems have been prepared and studied.

The films have been prepared using the spin-coating technique and have been deposited on glass substrates, using a spin velocity of 4500 rpm for 40 sec. Some of the spin-coated films have been also annealed at 170 ^oC for 1 hour, while in all cases, the film thickness was kept small (e.g. of the order of few nm) in order to keep linear aborption low. In Fig. 7, some representative UV-Vis-NIR absorption spectra of the prepared films are presented.

View Article Online
DOI: 10.1039/C3RA46132G

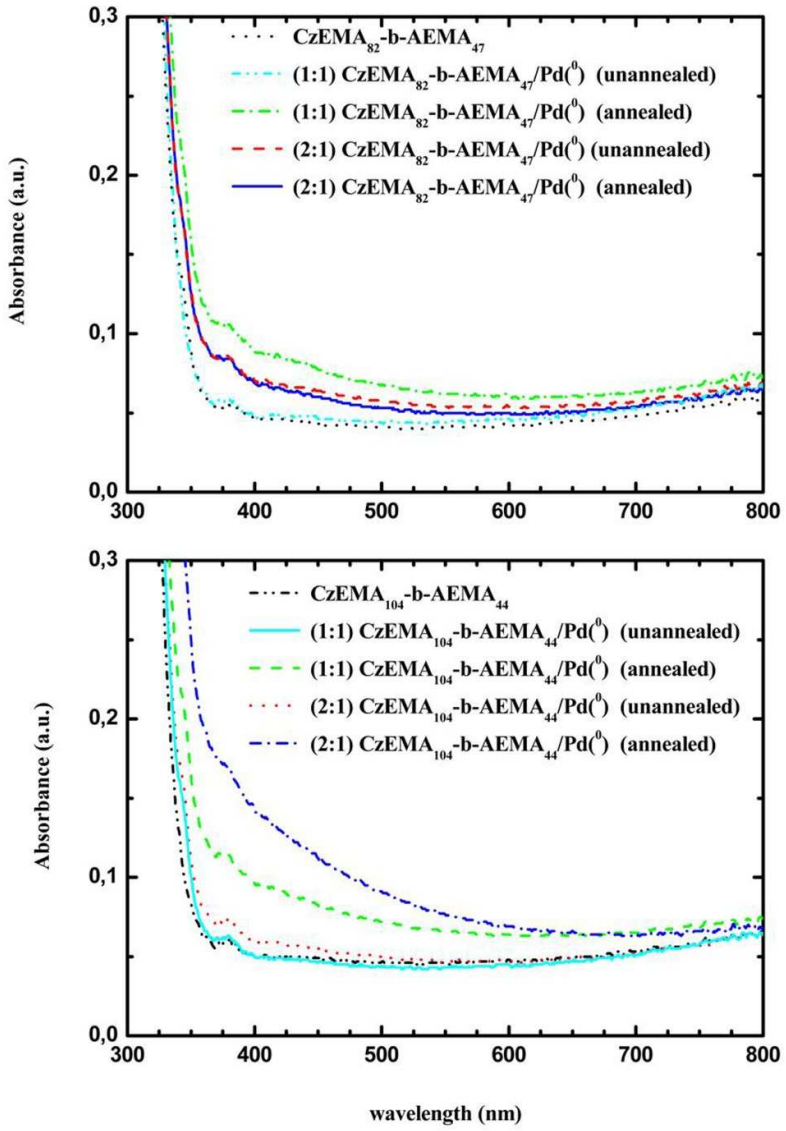

Fig. 7 UV-Vis-NIR absorption spectra of annealed and non-annealed thin films of Pd-polymer nanohybrids deposited on glass substrates *via* spin-coating.

The "divided" Z-scans of two representative films, namely of 1:1 CbzEMA$_{104}$-*b*-AEMA$_{44}$ and 2:1 CbzEMA$_{82}$-*b*-AEMA$_{47}$ non-annealed films obtained under 35 ps, 532 nm laser excitation are presented in Fig. 8a and 8c. The incident laser energy used was 6.8 μJ. As shown, both films displayed a "peak-valley" transmission

View Article Online
DOI: 10.1039/C3RA46132G

configuration, indicative of negative sign nonlinear refraction, similar to what has been found in the Z-scan studies of the micellar solutions. The corresponding "open-aperture" Z-scans, also shown in Fig. 8b and 8d, displayed negligible nonlinear absorption. In fact, the nonlinear absorption of the micellar nanohybrid-derived thin films has become observable at incident laser energies higher than 12 μJ, where however, nonlinear refraction started to saturate, thus preventing the accurate determination of the NLO parameters. In addition, analogous Z-scan measurements performed using 1064 nm laser excitation did not reveal any measurable NLO response for incident laser energy up to 50 μJ, where ablation started to become observable.

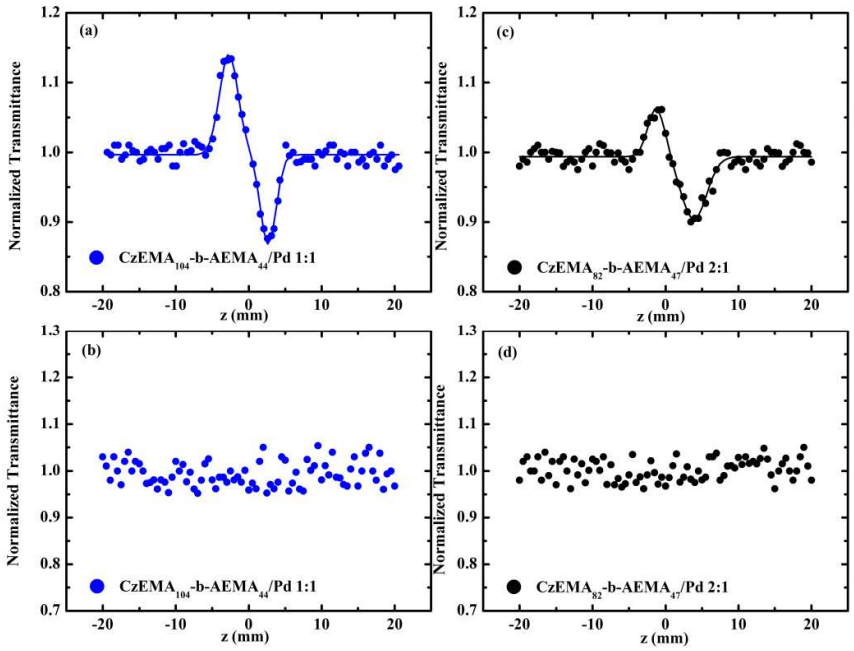

Fig. 8 "Divided" (a), (c) and "open-aperture" (b), (d) Z-scans of thin films generated *via* spin-coating of two different Pd-containing micellar systems, obtained using 6.8 μJ, 35 ps, 532 nm laser excitation.

From the absorption spectra of the Pd-containing micellar systems (in solution and/or in thin films) shown in Figures 5 and 7, it becomes clear that their featureless character in the 350 to 800 nm spectral region, does not provide any evidence of the

View Article Online
DOI: 10.1039/C3RA46132G

presence of surface plasmon resonance (SPR). The very weak shoulder at 380 nm (in the films' spectra) is most probably correlated with the presence of Pd(II) complexes, that have not been entirely reduced to Pd(^{0}). Similar featureless absorption spectra have been also reported by two other groups[46,47] exploring size control strategies of polyhedral Pd NPs and self-organisation issues. The same situation has been reported recently in the case of Pd-containing LauMA$_x$-*b*-AEMA$_y$ micellar systems[29] where (in the UV-Vis absorption spectra of the solutions) two broad absorption features apperring at 350 and 400 nm were attributed to Pd(II) complexes, not been entirely reduced to Pd(^{0}).

In contrast to the above, some other studies have reported the observation of Pd surface plasmon resonance feature, although often the findings are rather conflicting. In the case of Pd nanoparticles with diameters of a few nm found in colloidal suspensions[19,45], the SPR has been reported at 245 nm and 305 nm, while in the case of similar size Pd nanoparticles incorporated in the pores of silica glasses[48], the SPR peak has been reported at 320 nm. Furthermore, in another study, the SPR peak of 8 nm sized Pd nanocubes coated with polyvinylpyrrolidone (PVP) has been reported lying between 200 and 240 nm, while for larger size nanocubes, c.a. 25 and 50 nm, the SPR has been reported to be at 330 and 390 nm respectively[49.] Finally, in another study investigating the shape-controlled synthesis of Pd icosahedra NPs[50] the SPR peak has been observed to lie at about 286 nm.

Based on the above, it becomes probable that the large absorption below 350 nm of the Pd-containing micellar systems studied in this work, due to the block copolymers, might prevent the clear and unambiguous observation of the SPR, in case it is located in this spectral area. Nevertheless, the exact position of the SPR of Pd NPs is still not certain, in the sense that the various synthetic protocols result in NPs having different shapes and dimensions, affecting strongly the position and the spectral width of SPR[49]. Moreover, the use of surfactants and/or other chemicals (e.g., protective layers, solvent, etc) can further complicate the situation as their absorption may prevent the observation of the SPR peak as well.

Taking into account our experimental findings and considering the absence of the SPR in the visible and that no strong transitions occur in the visible part of the absorption spectrum, the observed enhancement could be explained in terms of a two-

View Article Online
DOI: 10.1039/C3RA46132G

photon process. In fact, such a situation has been previously considered by several groups investigating multiphoton processes in metallic nanoparticles[51,52]. Among those, in a recent work, studying the NLO absorption and refraction of Pd NPs, the authors attributed their experimental findings to such processes[53]. In fact, they have suggested that the two-photon process originated from the interband transitions between the *d* band and *s-p* conduction band of the Pd. Therefore, in the present work, in order for two 532 nm photons to be absorbed, the SPR should lie in the UV region. In addition, since similar enhancement, although weaker, can also be achieved under near resonant conditions, the SPR can be placed in a relatively larger spectral region extended c.a. from about 220 to 290 nm, according to the results reported by several literature reports as discussed above. In total, based on the present findings, the SPR of the Pd-containing micellar systems cannot be located with better accuracy. However, further work is in progress, using variable wavelength laser source, in order to detect the position of the SPR of these Pd-containing micellar systems.

4. Conclusions

In the present work a versatile synthetic route was employed for the preparation of Pd-containing micellar nanohybrid systems making use of new, well-defined, methacrylate-based amphiphilic block copolymers comprised of carbazole and β-ketoester side-chain functionalities. These micellar nanohybrids could be of great interest for optoelectronics and other photonic applications, since the promotion of the confinement of metallic NPs within well-defined nanostructured domains, becomes a valuable tool for controlling their size and shape, therefore allowing for the tuning of their nonlinear optical response.

In that view, the NLO properties of the block copolymer-Pd micellar nanohybrids, both in solution and in thin films, have been thoroughly investigated using picosecond, visible and infrared laser excitation. Their NLO response has been found to be larger under visible than under infrared excitation. In particular, negative sign NLO refraction (i.e. self-defocusing) has been observed under visible excitation, while positive sign NLO refraction (i.e. self-focusing) has been observed in the case of infrared excitation, while under both excitation wavelengths, positive sign NLO absorption has been found. In all cases, no sign of SPR peak has been observed in the

View Article Online
DOI: 10.1039/C3RA46132G

spectral range from 350 to 1100 nm. This fact, together with the larger NLO optical response of the Pd-containing micellar systems under 532 nm excitation, suggest that the SPR of the Pd nanoparticles should be located below 350 nm and most probably in the spectral region 220 to 290 nm, allowing two-photon resonant or near resonant conditions to occur, resulting in the enhancement of the NLO response under visible excitation.

Acknowledgements

This work has received partial financial support from the Research Promotion Foundation (RPF) of Cyprus (Program Technology/THEPIS/0308(BE)/06). We thank Dr. Rodica, P. Turcu (National Institute for Isotopic and Molecular Technologies, Cluj-Napoca, Romania) for the TEM analyses and the A. G. Leventis Foundation for a generous donation that enabled the purchase of the NMR spectrometer of the University of Cyprus. This research has been also co-financed by the European Union (European Social Fund – ESF) and Greek national funds through the Operational Program "Education and Lifelong Learning" of the National Strategic Reference Framework (NSRF) - Research Funding Programs: THALIS and Heracleitus II. Investing in knowledge society through the European Social Fund.

View Article Online
DOI: 10.1039/C3RA46132G

References

1 E. Bundgaard and F. C. Krebs, *Macromolecules*, 2006, **39**, 2823.

2 X. He, F. Gao, G. Tu, D. Hasko, S. Hüttner, U. Steiner, N. C. Greenham, R. H. Friend and W. T. S. Huck, *Nano Lett.*, 2010, **10**, 1302.

3 N. Tessler, V. Medvedev, M. Kazes, S. H. Kan and U. Banin, *Science*, 2002, **295**, 1506.

4 B. S. Ong, Y. Wu, Y. Li, P. Liu and H. Pan, *Chem. Eur. J.*, 2008, **14**, 4766.

5 X. Liu and M. Jiang, *Angew. Chem.*, 2006, **118**, 3930.

6 C. Gu, Y. Xu, Y. Liu, J. J. Pan, F. Zhou and H. He, *Opt. Mater.*, 2003, **23**, 219.

7 H. Chun, W. J. Joo, N. J. Kim, I. K. Moon and N. Kim, *J. Appl. Polym. Sci.*, 2003, **89**, 368.

8 J. V. Grazuleviciu, P. Strohriegl, J. Pielichowski and K. Pielichowski, *Prog. Polym. Sci.*, 2003, **28**, 1297.

9 I. Fuks, B. Derkowska, B. Sahraoui, S. Niziol, J. Sanetra, D. Bogdal and J. Pielichowski, *J. Opt. Soc. Amer. B*, 2002, **19**, 89.

10 Y. Zhang, M. Yamakado, T. Wada and H. Sasabe, *J. Photopolym. Sci. Technol.*,m1993, **6**, 201.

11 X. Zhan, Y. Liu, D. Zhu, X. Liu, G. Xu and P. Ye, *Chem. Phys. Lett.*, 2002, **362**, 165.

12 R. A. Ganeev, *J. Opt. A: Pure Appl. Opt.*, 2005, **7**, 717.

13 E. Xenogiannopoulou, K. Iliopoulos, S. Couris, T. Karakouz, A. Vaskevich and I. Rubinstein, *Adv. Funct. Mater.*, 2008, **18**, 1281.

14 H. Zhao, E. P. Douglas, B. S. Harrison and K. S. Schanze, *Langmuir*, 2001, **17**, 8428.

15 C. C. Wang, A. L. Chen and I. H. Chen, *J. Coll. Interf. Sci.*, 2006, **293**, 421.

16 C. T. Black, R. Ruiz, G. Breyta, J. Y. Cheng, M. E. Colburn, K. W. Guarini, H. C. Kim and Y. Zhan, *IBM J. Res. Dev.*, 2007, **51**, 605.

17 T. Goodson, O. Varnavski and Y. Wang, *Int. Rev. Phys. Chem.*, 2004, **23**, 109.

18 R. B. Grubbs, *Polym. Rev.*, 2007, **47**, 197.

19 R. A. Ganeev, M. Suzuki, M. Baba, M. Ichihara and H. Kuroda, *J. Appl. Phys.*, 2008, **103**, 063102-1.

20 J. Ebothe, I. V. Kityk, G. Chang, M. Oyama and K. J. Plucinski, *Physica E*, 2006, **35**, 121.

21 H. Zeng, Y. Yang, X. Jiang, G. Chen, J. Qiu and F. Gan, *J. Cryst. Growth*, 2005, **280**, 516.

View Article Online
DOI: 10.1039/C3RA46132G

22 J. Durand, E. Teuma and M. Gomez, *Eur. J. Inorg. Chem.*, 2008, **2008**, 3577.

23 M. Yamauchi and H. Kitagawa, *Synth. Met.*, 2005, **153**, 353.

24 J. S. Noh, J. M. Lee and W. Lee, *Sensors*, 2011, **11**, 825.

25 C. Drake, S. Deshpande, D. Bera and S. Seal, *Int. Mater. Rev.*, 2007, **52**, 289.

26 S. Föster and M. Antonietti, *Adv. Mater.*, 1998, **10**, 195.

27 H. Schlaad, T. Krasia and C.S. Patrickios, *Macromolecules*, 2001, **34**, 7585.

28 T. Krasia, R. Soula, H. Börner and H. Schlaad, *Chem. Commun.*, 2003, **9**, 538.

29 K. Iliopoulos, G. Chatzikyriakos, M. Demetriou, T. Krasia-Christoforou and S. Couris, *Opt. Mater.*, 2011, **33**, 1342.

30 J. Chiefari, Y. K. Chong, F. Ercole, J. Krstina, J. Jeffery, T. P. T. Le, R. T. A. Mayadunne, G. F. Meijs, C. L. Moad, G. Moad, E. Rizzardo and S. H. Thang, *Macromolecules*, 1998, **31**, 5559.

31 T. Krasia and C. S. Patrickios, *Polymer*, 2002, **43**, 2917.

32 P. Zhao, Q. D. Ling, W. Z. Wang, J. Ru, S. B. Li and W. Huang, *J. Polym. Sci. Part A: Polym. Chem.*, 2007, **45**, 242.

33 Y. S. Cho, J. S. Lee and G. Cho, *Polymer*, 2002, **43**, 1197.

34 M. Ohoka, J. Kuno, K. Yamashita, H. Ohkita, S. Ito, Y. Tsujii and T. Fukuda, *Kobunshi Ronbunshu*, 2002, **59**, 421.

35 T. P. T. Le, G. Moad, E. Rizzardo, S. H. Thang, PCT. Int. Appl. 1998, WO 9801478 A1 980115.

36 S. Ito, S. Ohmori and M. Yamamoto, *Macromolecules*, 1992, **25**, 185.

37 F. S. Du, Z. C. Li, W. Hong, Q. Y. Gao and F. M. Li, *J. Polym. Sci.: Part A: Polym. Chem.*, 2000, **38**, 679.

38 M. Sheik-Bahae, A. A. Said, T. H. Wei, D. J. Hagan and E. W. Van Stryland, *IEEE J. Quant. Electr.*, 1990, **26**, 760.

39 E. Koudoumas, M. Konstantaki, A. Mavromanolakis, X. Michaut, S. Couris and S. Leach, *J. Phys. B: At. Mol. Opt. Phys.*, 2001, **34**, 4983.

40 S. Couris, E. Koudoumas, A. A. Ruth and S. Leach, *J. Phys. B: At. Mol. Opt. Phys.*, 1995, 2, 4537.

41 L. M. Bronstein, S. N. Sidorov, A. Y. Gourkova, P. M. Valetsky, J. Hartmann, M. Breulmann, H. Cölfen and M. Antonietti, *Inorg. Chim. Acta*, 1998, 280, 348.

42 R. Gvishi, T.H. McMillian, D.J. Hagan, E.W. Van Stryland, K.J. Schafer, S, Yao, K.D. Belfield, *Proceedings of SPIE-The International Society for Optical Engineering 5934* 2005, art. no. 59340C, 1-8.

43 G. R. Meredith, B. Buchalter and C. Hanzlik, *J. Chem. Phys.*, 1983, **78**, 1543.

44 I. Papagianoulli, M. Demetriou, G. Chatzikyriakos, K. Iliopoulos, T. Krasia-Christoforou and S. Couris, *Opt. Mater.*, 2013, **36**, 123.

View Article Online
DOI: 10.1039/C3RA46132G

45 R. A. Ganeev, G. S. Boltaev, R. I. Tugushev and T. Usmanov, *Appl. Phys. B*, 2010, **100**, 571.

46 Q. Zhang, J. Xie, J. Yang and J.Y. Lee, *ACS Nano*, 2009, **3**, 139.

47 F. P. Zamborini, S. M. Gross and R. W. Murray, *Langmuir*, 2001, **17**, 481.

48 T. B. Boitsova, V. V. Gorbunova and Y. M. Voronin, *J. Opt. Technol.*, 2001, **68**, 789.

49 Y. Xiong, J. Chen, B. Wiley, Y. Xia, Y. Yin and Z.-Y. Li, *Nano Lett.*, 2005, **5**, 1237.

50 Y. Yu, Y. Zhao, T. Huang and H. Liu, *Pure Appl. Chem.*, 2009, **81**, 2377.

51 M. Fierz, K. Siegmann, M. Scharte and M. Aeschlimann, *Appl. Phys. B*, 1999, **68**, 415.

52 R. Philip, G. Ravindra Kumar, N. Sandhyarani and T. Pradeep, *Phys. Rev. B*, 2000, **62**, 13160.

53 G. Fan, S. Qu, Q. Wang, C. Zhao, L. Zhang and Z. Li, *J. Appl. Phys.*, 2011, **109**, 023102.

View Article Online
DOI: 10.1039/C3RA46132G

TOC Figure